BBA - Molecular Cell Research 1867 (2020) 118761

Contents lists available at ScienceDirect

BBA - Molecular Cell Research

journal homepage: www.elsevier.com/locate/bbamcr

Expression of nuclear XIAP associates with cell growth and drug resistance and confers poor prognosis in breast cancer

Deborah Delbue[a,1], Bruna S. Mendonça[a,b,1], Marcela C. Robaina[a], Lauana G.T. Lemos[a], Pedro I. Lucena[c], João P.B. Viola[c], Lídia M. Magalhães[d], Susanne Crocamo[e], Caio A.B. Oliveira[f], Felipe R. Teixeira[f], Raquel C. Maia[a], Gabriela Nestal de Moraes[a,*]

[a] Laboratório de Hemato-Oncologia Celular e Molecular, Programa de Hemato-Oncologia Molecular, Instituto Nacional de Câncer (INCA), Praça da Cruz Vermelha, 23, 6° andar, Centro, 20 230 130 Rio de Janeiro, RJ, Brazil
[b] Programa de Pós-Graduação Stricto Sensu em Oncologia, INCA, Rua André Cavalcanti, 37, 5° andar, Centro, 20 230 050, RJ, Brazil
[c] Programa de Imunologia e Biologia Tumoral, INCA, Rua André Cavalcanti, 37, 5° andar, Centro, 20 230 050, RJ, Brazil
[d] Divisão de Anatomia Patológica, INCA, Rua Cordeiro da Graça, 156, Santo Cristo, 20 220 400 Rio de Janeiro, Brazil
[e] Núcleo de Pesquisa Clínica, Hospital de Câncer III, INCA, Rua Visconde de Santa Isabel, 274, Vila Isabel, 20 560 120 Rio de Janeiro, Brazil
[f] Departamento de Genética e Evolução, Universidade Federal de São Carlos, Rodovia Washington Luís, km 235, 13 560 300 São Carlos, São Paulo, Brazil

ARTICLE INFO

Keywords:
XIAP
Subcellular localization
Breast cancer
Drug resistance
Prognosis

ABSTRACT

Evasion from apoptosis is one of the hallmarks of cancer. X-linked inhibitor of apoptosis protein (XIAP) is known to modulate apoptosis by inhibiting caspases and ubiquitinating target proteins. XIAP is mainly found at the cytoplasm, but recent data link nuclear XIAP to poor prognosis in breast cancer. Here, we generated a mutant form of XIAP with a nuclear localization signal ($XIAP^{NLS\text{-}C\text{-}term}$) and investigated the oncogenic mechanisms associated with nuclear XIAP in breast cancer. Our results show that cells overexpressing $XIAP^{\Delta RING}$ (RING deletion) and $XIAP^{NLS\text{-}C\text{-}term}$ exhibited XIAP nuclear localization more abundantly than $XIAP^{wild\text{-}type}$. Remarkably, overexpression of $XIAP^{NLS\text{-}C\text{-}term}$, but not $XIAP^{\Delta RING}$, conferred resistance to doxorubicin and increased cellular proliferative capacity. Interestingly, Survivin and c-IAP1 expression were not associated with XIAP oncogenic effects. However, NFκB expression and ubiquitination of K63, but not K48 chains, were increased following $XIAP^{NLS\text{-}C\text{-}term}$ overexpression, pointing to nuclear signaling transduction. Consistently, multivariate analysis revealed nuclear, but not cytoplasmic XIAP, as an independent prognostic factor in hormone receptor-negative breast cancer patients. Altogether, our findings suggest that nuclear XIAP confers poor outcome and RING-associated breast cancer growth and chemoresistance.

1. Introduction

Breast cancer is the most common malignancy within women in Brazil and worldwide. Despite improvements in therapeutic options over the last decades, overall survival for advanced breast cancer remains disappointing. The acquisition of drug resistance accounts for, at least in part, treatment failure and eventual relapse in these patients. The efficacy of chemotherapeutic agents relies mainly on their ability to sensitize cancer cells towards programmed cell death. X-linked IAP (XIAP) is the prototype member of the inhibitor of apoptosis proteins (IAP), family known to negatively regulate the apoptotic cascade through a wide diversity of mechanisms [1]. The mechanisms underlying XIAP antiapoptotic function have been initially attributed to its BIR domain-dependent binding and direct inhibition of caspases [2]. However, XIAP presents a RING domain in its C-terminal, which exhibits E3 ubiquitin ligase activity and thus, regulates stability of itself [3] and proapoptotic proteins such as caspase-3 [4] and Smac [5]. Although XIAP expression is detected in non-neoplastic tissues [6], XIAP overexpression is observed in a wide variety of tumor types, which has been shown to counteract drug-induced cell death *in vitro* and to associate with poor outcome in cancer patients [7]. Regarding cellular distribution, XIAP expression is mainly cytoplasmic, but can present nuclear localization in specific cell types [6]. We have recently assessed XIAP expression in breast cancer patient samples and demonstrated that

* Corresponding author at: Laboratório de Hemato-Oncologia Celular e Molecular, Programa de Hemato-Oncologia Molecular, Instituto Nacional de Câncer (INCA), Praça da Cruz Vermelha, 23, 6° andar, Centro, 20 230 130 Rio de Janeiro, RJ, Brazil.
E-mail address: gabinestal@yahoo.com.br (G. Nestal de Moraes).
[1] The authors equally contributed to this study.

https://doi.org/10.1016/j.bbamcr.2020.118761
Received 7 February 2020; Received in revised form 5 May 2020; Accepted 27 May 2020
Available online 30 May 2020

it can be detected in both nuclear and cytoplasmic subcellular compartments [8]. Also, we have found that co-expression of nuclear XIAP, but not cytoplasmic, with Survivin and FOXM1 oncogenic proteins, associates with shorter survival [8]. Consistently, nuclear XIAP had been previously described as an independent prognostic biomarker in a different cohort of breast cancer patients [9]. However, the mechanisms underlying XIAP oncogenic functions at the nucleus of breast cancer cells remain unexplored. Here, we generated a mutant form of XIAP with an insertion of the nuclear localization signal (NLS) of SV40 T antigen ($XIAP^{NLS\ C\text{-}term}$) in its sequence and investigated how XIAP contributes to aggressive features in this model. We report that $XIAP^{NLS\ C\text{-}term}$ and $XIAP^{\Delta RING}$ transfectants localize in the nucleus of breast cancer cells expressing basal levels of cytoplasmic XIAP. Notably, ectopic expression of $XIAP^{NLS\ C\text{-}term}$, but not $XIAP^{\Delta RING}$, associates with a chemoresistance phenotype and increased growth capacity. Interestingly, expression of p50 subunit of NFκB and ubiquitination in K63 chains were induced following transfection with $XIAP^{NLS\ C\text{-}term,}$ with no significant changes in K48 chains, an effect similarly dependent on the RING domain of XIAP. Finally, nuclear expression of XIAP was found to be an independent prognostic factor in hormone receptor (HR)-negative breast cancer patients, further confirming the biological relevance of these findings.

2. Materials and methods

2.1. Breast cancer patients' samples

The expression and localization of XIAP in breast cancer patients' samples was analyzed by immunohistochemistry (IHC) in a previous study [8]. Briefly, the mean percentage and intensity of stained cells was evaluated and a score for XIAP staining was calculated. The intensity of staining was considered as follows: 0 = no expression, 1 = weak, 2 = moderate, 3 = strong. The percentage of positively stained cells was scored as: 0 = no cells, 1 = 1–9%, 2 = 10–40%, 3 = 50–79%, 4 = 80–100%. For each sample, a total score for nuclear and cytoplasmic staining was calculated by multiplying the intensity score by the percentage score, with resulting scores ranging from 0 to 12. We considered 0–2 as negative and 3–12 as positive scores. In this study, data concerning XIAP expression and localization was reanalyzed particularly with regard to patient stratification within breast cancer subgroups with distinct clinical and pathological parameters. This study was approved by our Institutional Ethics Committee, under the protocol number 153/09.

2.2. Cell lines and drug treatment

In this study, we used MCF-7 (non-invasive, HR positive), T47D (non-invasive, HR positive), MDA-MB-231 (invasive, triple negative), BT549 (invasive, triple negative) and HB4a (non-neoplastic cell line originated from luminal breast cells) cell lines as models. Except for BT549 cells, which were cultured in RPMI 1640 medium, the cell lines were cultured in DMEM medium (Gibco) supplemented with 10% inactivated fetal bovine serum (FBS) and 1 μL/mL penicillin/streptomycin (Life Technologies). Non-neoplastic HB4a cells were cultured in DMEM medium supplemented with 10% heat-inactivated FBS (Gibco), 1 μL/mL penicillin/streptomycin and 5 μM hydrocortisone and insulin. The cell lines were kept in a humidified atmosphere at 37 °C and 5% CO_2. Cells in exponential growth were treated with doxorubicin (Fauldoxo®-Libbs Pharmaceuticals Ltda, São Paulo) and paclitaxel (Paclitaxel® - Accord Pharmaceuticals Ltda, São Paulo) at increasing concentrations and time-points.

2.3. Plasmid construction

Plasmid vectors pEBB (empty vector), pEBB-HA-$XIAP^{wild\ type}$, pEBB-HA-$XIAP^{H467A}$ (loss of ubiquitin E3 ligase function) and pEBB-HA-$XIAP^{\Delta RING}$ (deletion of the RING domain) were kindly provided by Professor Colin Duckett's laboratory [10]. pEBB-HA-$XIAP^{NLS\ N\text{-}term}$ and pEBB-HA-$XIAP^{NLS\ C\text{-}term}$ vectors were constructed by fusing oligonucleotides containing the NLS coding sequence of the SV40 virus T antigen (amino acid sequence: SPKKKRKVEAS) to the 5′ or 3′ XIAP cDNA, respectively. To construct the $XIAP^{NLS\ N\text{-}term}$ vector, the NLS sequence was inserted between the HA tag and the XIAP initiation codon in the $XIAP^{wild\ type}$ vector, using the *Bam*HI and *Bgl*II enzymes. To construct the $XIAP^{NLS\ C\text{-}term}$ vector, the XIAP stop codon was removed by PCR amplification followed by subcloning to the pEBB vector using the *Eco*RV and *Cla*I enzymes and the NLS sequence was inserted in the 3′ from the XIAP cDNA using *Cla*I and *Not*I restriction enzymes. All constructs were confirmed by restriction enzyme mapping and DNA sequencing (Applied Biosystems), using primer sequences available at Supplementary Table 1.

2.4. Transfection of XIAP vectors into breast cancer cells

Cell transfections with the plasmid vectors: pEBB, HA-$XIAP^{wild\ type}$, HA-$XIAP^{H467A}$, HA-$XIAP^{\Delta RING}$, HA-$XIAP^{NLS\ N\text{-}term}$ and HA-$XIAP^{NLS\ C\text{-}term}$ were conducted using the Lipofectamine 2000 reagent (Invitrogen), according to manufacturer's instructions. After 24 h of transfection, cells were trypsinized and reseeded for subsequent experiments. XIAP overexpression was confirmed by Western blotting.

2.5. Measurement of metabolic cell viability

The MTT assay was performed for measurement of drug-mediated changes in cell viability. Briefly, 10^4 cells were plated in 96-well plates and left to adhere for 24 h. After 24, 48 and 72 h treatment with increasing concentrations of doxorubicin, cells were submitted to the MTT assay, as previously described [11]. Alternatively, cells transfected with XIAP expression vectors had their growth profile assessed in a 72 h kinetics, for direct comparison. The experiments were done in triplicates and the mean values of optical densities at 570 nm (EZ Read 400 Microplate Reader, Biochrom) from each experiment were normalized to 100%.

2.6. Clonogenic assay

A total of 2×10^3 cells was plated in 6-well plates and treated with doxorubicin and paclitaxel after 24 h adherence. Following 24 or 48 h of treatment, drugs were removed and cells maintained in drug-free media until colony formation (approximately 14 days). Colonies were fixed in absolute ethanol, stained with 0.5% crystal violet and air-dried. Dilution in 33% glacial acetic acid solution was performed and the optical density was measured at 595 nm. Optical densities in control untreated cells were normalized to 1 for comparison within experiments. The clonogenicity was assessed in, at least, three independent experiments.

2.7. DNA content flow cytometry analysis of cell cycle distribution and cell death

Cells were transfected with XIAP expression vectors and a total of 5×10^5 cells were left to adhere onto T25 flasks for 24 h. Cells were then harvested and cell cycle distribution was assessed by DNA content analysis following addition of 50 μg/mL propidium iodide (PI) and ribonuclease A (100 μg/mL). Alternatively, XIAP-overexpressing cells were treated with doxorubicin and had cell death-associated DNA fragmentation estimated by the percentage of hypodiploid population in the sub-G0/G1 phase. Fluorescence was measured by flow cytometry using a FACSCalibur (BD Beckton Dickinson FACSCalibur). Data analysis was performed using the Summit 4.3v software.

2.8. Crystal violet staining

Following transfections, cells were reseeded in 96-well plates for 24 h and treated with doxorubicin for 24 h. Cells were fixed in 100% ethanol and stained with 0.05% crystal violet at 24 h after adhesion or at 24 h of drug treatment. Dilution was performed in 100% methanol and optical densities were measured at 595 nm in a microplate reader (EZ Read 400 Microplate Reader, Biochrom).

2.9. Western blotting

For protein content analysis, pellets of 2×10^6 cells were washed three times in phosphate buffered saline (PBS), lysed in Invitrogen cell extraction buffer (Eugene, OR, Carlsbad, CA, US) and quantified using the Bio-Rad protein assay solution (Life Science Research, Hercules, CA). Antibodies for XIAP (1:1000 dilution; Cell Signaling), Survivin (1:1000 dilution; Cell Signaling), cIAP-1 (1:1000 dilution; Cell Signaling), p50/p105 (1:1000 dilution, Cell Signaling), p65 (1:1000 dilution, Cell Signaling), K48 (1:1000 dilution, Cell Signaling), K63 (1:1000 dilution, Cell Signaling), HA-tag (1:500 dilution; Cell Signaling), GAPDH (1:10000 dilution, Sigma-Aldrich), Hsc70 (1:1000 dilution; Santa Cruz) and β-tubulin (1:1000 dilution; Santa Cruz), and Lamina B (1:300 dilution; Calbiochem) were used. Mouse and rabbit secondary antibodies were purchased from Sigma-Aldrich (1:20,000 dilution). Protein bands were developed using the Clarity Max™ substrate (Western ECL Substrate – BioRad Laboratories, Hercules, CA, US) and detected using the C-DiGit blot scanner (Li-cor Biociences, Lincoln, Nebraska, USA).

2.10. Subcellular fractioning

The NE-PER (Nuclear and Cytoplasmic Extraction Reagents, ThermoFisher Scientific) kit was used to isolate the cytoplasmic and nuclear fractions, according to manufacturer's instructions. XIAP levels were evaluated in each subcellular fraction by Western blotting. GAPDH and Hsc70 proteins were used as cytoplasmic marker and Lamina B, as a nuclear constitutive control.

2.11. Immunofluorescence and confocal microscopy

For analysis of XIAP subcellular localization, cells were fixed in 4% paraformaldehyde for 15 min at −20 °C, and washed with PBS, permeabilized and blocked with 1% BSA and 0.1% Triton X-100 in PBS for 30 min. Then, cells were incubated in 50 mM NH_4Cl for 15 min and, subsequently, in anti-XIAP (1:20; Santa Cruz) and anti-HA (1:50; Cell Signaling) primary antibodies overnight at −4 °C. On the following day, cells were incubated for 1 h at room temperature with appropriate Alexa Fluor secondary antibodies (1:200; Molecular Probes) and stained with DAPI for 10 min, after which glass slides were washed and mounted using n-propyl-gallate. Cell staining was visualized with a confocal laser scanning microscope (FV10i-O), and the images were analyzed using the FV10-ASW software (Olympus).

2.12. NF-κB luciferase reporter assay

HEK293 cells stably expressing pBIIx-luc described in [12] were kindly provided by Dr. Dario Zamboni (Department of Cellular and Molecular Biology, Faculty of Medicine of Ribeirao Preto, University of Sao Paulo). They were cultured in 96-well plates at 5×10^5 cells/well, and after 24 h, transfected with 75 ng of each plasmid (pEBB, HA-$XIAP^{wild\ type}$, HA-$XIAP^{H467A}$, HA-$XIAP^{\Delta RING}$ and HA-$XIAP^{NLS\ C\text{-}term}$) and 1.5 ng of pCMV-Renilla luciferase control plasmid, with Lipofectamine 2000. After 24 h, cells were treated or not with 10 ng/mL TNF-α in serum deprived DMEM without phenol red (Gibco) for 12 h. Cells were lysed by Dual-Glo Luciferase assay kit (Promega), transferred to white 96-well Corning Costar® plates and Firefly and Renilla luciferase activity measurement were obtained in a SpectraMax i3 luminometer (Molecular Devices).

2.13. Statistical analysis

The SPSS 17.0 (SPSS for Windows, version 17.0, SPSS Inc.) software was used to perform the statistical analysis with the breast cancer patient samples. To estimate overall survival (OS), the Kaplan-Meyer curves were compared by the log-rank test. OS was defined as the time between diagnosis and death by any cause or censored at last follow-up. Multivariate anal + ysis by Cox proportional hazard models was performed to assess the independent prognostic impact of XIAP subcellular localization. The chi-square test was used to evaluate the association between the XIAP expression and localization with the patients' clinical-biological parameters. Paired Student's *t*-test or Two-way ANOVA were used to compare differences between means from different groups in experiments *in vitro*. All tests were two-sided and the value of $p < 0.05$ was considered statistically significant.

3. Results

3.1. XIAP expression is more abundantly found in the cytoplasm of breast-derived cell lines

XIAP expression has been widely reported in non-neoplastic tissues, where a predominant cytoplasmic localization has been found [6]. Although XIAP overexpression has been implicated in prognosis and response *in vitro* to chemotherapeutic agents, little is known on the subcellular distribution of XIAP in breast cancer cells. To address this issue, we initially analyzed XIAP expression and subcellular localization in a panel of breast-derived cell lines. For this purpose, we assessed cell lines originated from distinct molecular breast cancer subtypes along with a non-neoplastic breast model. Our results from Western blotting analysis of whole cell extracts show that breast-derived cell lines exhibited different levels of XIAP expression, which were found higher in the MDA-MB-231 cell line (Fig. 1A). When we performed subcellular fractionation and obtained cell extracts enriched for nuclear and cytoplasmic fractions, we found that all cell lines presented cytoplasmic localization of XIAP, irrespective of XIAP basal expression levels (Fig. 1B). We have also analyzed subcellular distribution of XIAP by confocal microscopy and observed that XIAP is mainly expressed in the cytoplasm of MCF-7 cells (Fig. 1C). These results suggest that breast-derived cell lines exhibit mainly cytoplasmic expression of XIAP.

3.2. $XIAP^{\Delta RING}$ and $XIAP^{NLS\ C\text{-}term}$ localize in both nuclear and cytoplasmic fractions in breast cancer cells

It has been previously described that a mutant form of XIAP, deleted for the RING domain ($XIAP^{\Delta RING}$), localized at the nucleus of colorectal cancer cells and induced cell growth, differently from its vector control $XIAP^{H467A}$, which lacks E3 ubiquitin ligase activity but localizes at the cytoplasm [13]. To understand the mechanisms underlying the oncogenic role of nuclear XIAP in breast cancer, we used these mutants as a tool to induce XIAP expression and evaluate its localization at cellular compartments. In addition, since XIAP does not present an NLS, we generated XIAP with an NLS at the N-terminal and C-terminal ends (Fig. 2A). Subsequently, we transfected XIAP constructs into MCF-7 cells and analyzed its expression in whole cell and fractioned extracts. Following 24 h post-transfection, we found that overexpression of all mutants resulted in cytoplasmic localization but only $XIAP^{\Delta RING}$ and $XIAP^{NLS\ C\text{-}term}$ mutants were more expressed and also abundantly localized at the nucleus (Fig. 2B and C). Interestingly, we could not find the same pattern of $XIAP^{NLS\ C\text{-}term}$ expression and localization in $XIAP^{NLS\ N\text{-}term}$-overexpressing cells, hence we did not proceed with $XIAP^{NLS\ N\text{-}term}$ mutant in subsequent experiments. To further establish the subcellular distribution of the transfectants, we immunolabelled

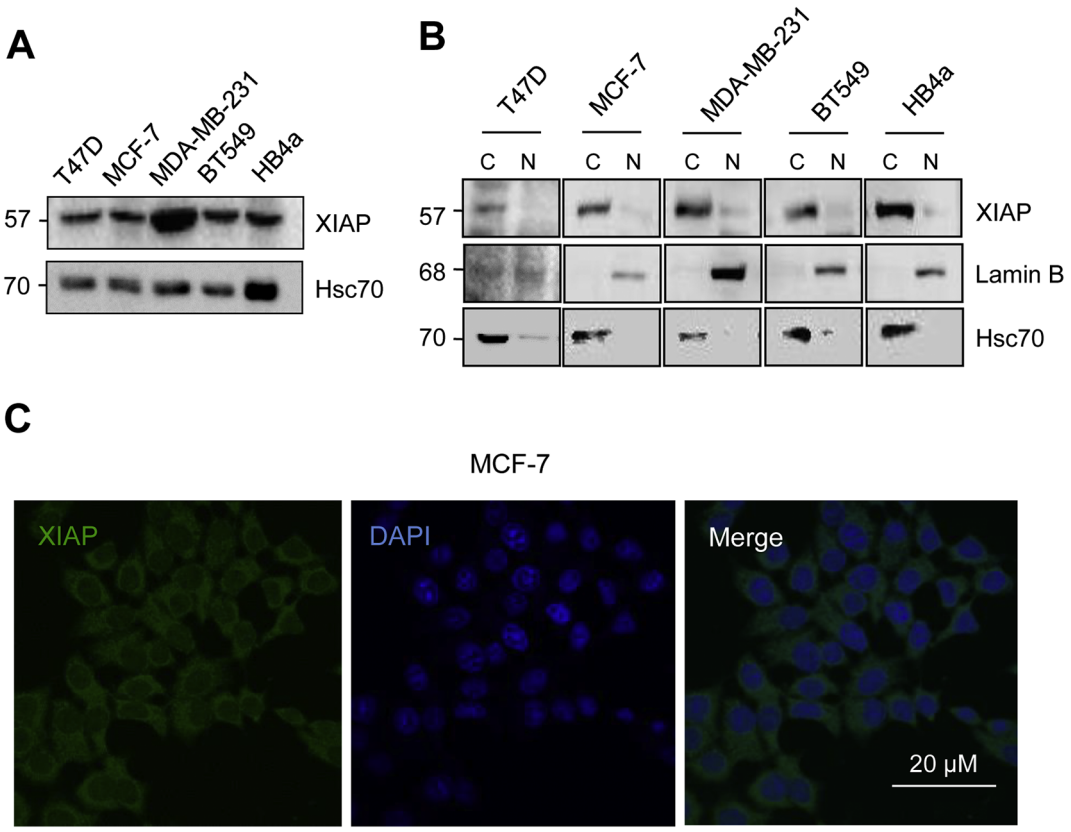

Fig. 1. Breast-derived cell lines exhibit predominantly cytoplasmic expression of XIAP. T47D, MCF-7, MDA-MB-231, BT549 and HB4a cells were left to adhere for 24 h and then had their cytoplasmic and nuclear fractions separated by the NE-PER kit (Thermoscientific). Subsequently, whole cell (A) and fractioned (B) lysates were subjected to the analysis of XIAP expression by Western blotting. Lamin B was used as a nuclear constitutive control, while Hsc70 as cytoplasmic constitutive control. C: cytoplasm; N: nucleus. (C). MCF-7 were seeded into slides and submitted to the immunofluorescence protocol for XIAP staining. Subcellular localization of XIAP was analyzed by confocal microscopy and nuclei were counterstained with DAPI. Scale bar: 20 μM.

cells overexpressing XIAP with anti-XIAP and anti-HA-tag antibodies and performed confocal microscopy analysis. The images show that nuclear XIAP expression co-localized with HA-tag-stained cells (Fig. 2D), validating our model of induced exogenous XIAP overexpression at the nucleus of breast cancer cells.

3.3. Ectopic expression of XIAP$^{NLS\ C\text{-}term}$, but not XIAP$^{\Delta RING}$, promotes breast cancer cell growth

Next, we functionally addressed the role of XIAP mutants in growth in breast cancer cells. For this purpose, we transfected MCF-7 cells with plasmids encoding the empty vector, the wild-type and the mutant forms of XIAP (Fig. 3A). After 24 h of transfections, we counted cells by trypan blue exclusion and found that XIAP$^{wild\text{-}type}$ and XIAP$^{\Delta RING}$ exhibited augmented cell number compared to the empty vector (Fig. 3B). Remarkably, the highest cell count was observed in XIAP$^{NLS\ C\text{-}term}$ cells, which exhibit XIAP expression levels comparable to XIAP$^{\Delta RING}$ cells (Fig. 3B). Short-term cell viability was similarly increased over a time-course of 24, 48 and 72 h following XIAP$^{NLS\ C\text{-}term}$ overexpression, comparatively with the other transfectants (Fig. 3C). We then assessed long-term viability of cells transfected with these constructs through clonogenic assay. Consistent with results from short-term cytotoxicity assays, XIAP$^{NLS\ C\text{-}term}$ overexpressing cells had the most pronounced clonogenicity capacity within XIAP variants, particularly comparing with XIAP$^{\Delta RING}$ cells presenting similar XIAP content (Fig. 3D). Of note, we found no changes in cell cycle distribution when comparing all transfectants (Fig. 3E and Supplementary Fig. 1), suggesting that differential pattern of proliferation is not resulted from a phase arrest. DNA content analysis also revealed a low percentage of sub-G0/G1 cells following transfection with XIAP variants (Supplementary Fig. 2), indicating that differences in cell number are not a result of fewer cells undergoing cell death. These findings suggest that the induction of XIAP expression in the nucleus is associated with breast cancer cell growth, an effect that requires the RING domain of XIAP.

3.4. XIAP protects breast cancer cells from doxorubicin-induced cell death in a RING domain-dependent manner

XIAP overexpression has been widely implicated in cancer drug resistance, mainly through its BIR domains through which it exerts its caspase-inhibitory activities [14]. However, the impact of XIAP subcellular localization in the response of breast cancer cells to the cytotoxic effects of chemotherapeutic agents has not been investigated. To address this issue, MCF-7 cells transfected with XIAP variants were exposed to 24 h clinically relevant concentrations of doxorubicin, a chemotherapeutic agent commonly used to treat breast cancer. Our results show that MCF-7 cells overexpressing mutant forms of XIAP presented distinct profiles of response to doxorubicin (Fig. 4A). Notably, overexpression of XIAP$^{NLS\ C\text{-}term}$, but not XIAP$^{\Delta RING}$, rendered cells less sensitive to doxorubicin treatment (Fig. 4B). Confirming these data, analysis of clonogenic assays revealed that transfection with the XIAP$^{NLS\ C\text{-}term}$ vector prevented, at least in part, cells from doxorubicin-induced inhibition of colony formation (Fig. 4C), differently from the other vectors. Moreover, our cell death analysis failed to find differences between XIAP expression vectors upon a 24 h doxorubicin exposure (Supplementary Fig. 2), probably because later steps of doxorubicin-induced apoptotic cascade are known to occur in a time-dependent manner. Interestingly, breast-derived cell lines which exhibit XIAP expression exclusively in the cytoplasm were shown to present a sensitive phenotype towards doxorubicin in short (Supplementary

Fig. 3) and long-term (Supplementary Fig. 4A-D) viability assays. Also, doxorubicin treatment did not change the subcellular localization of XIAP in both MCF-7 and MDA-MB-231 cell lines (Supplementary Fig. 5A and B). These findings were confirmed in MCF-7 cells treated with paclitaxel, another chemotherapeutic agent used in breast cancer treatment, where no changes in XIAP localization were observed after treatment (Supplementary Fig. 6A and B). Altogether, these results suggest that while cytoplasmic XIAP associates with a favorable response to drug treatment, XIAP accumulation in the nucleus of breast cancer cells is linked to a drug resistance phenotype.

3.5. XIAP$^{NLS\ C\text{-}term}$-mediated effects are associated with increased p50 content and polyubiquitination of K63, but not K48-linked chains

Next, we went on to explore the mechanisms underlying XIAP-induced oncogenic effects. We initially analyzed the expression of proteins known to cross-talk with XIAP to counteract apoptosis, such as the NF-κB transcription factor [15] and other members of IAP family [16]. To investigate the involvement of these signaling pathways in XIAP$^{NLS\ C\text{-}term}$-mediated effects, we then obtained whole cell extracts from XIAP transfectants and compared protein expression in XIAP$^{NLS\ C\text{-}term}$ and XIAP$^{\Delta RING}$ overexpressing cells, which present nearly similar levels of XIAP. Although p50 and p105 subunits of NF-κB had their expression remarkably increased in XIAP$^{NLS\ C\text{-}term}$ cells, we found no difference in the p65 subunit, neither in Survivin or c-IAP1 expression in XIAP$^{NLS\ C\text{-}term}$ and XIAP$^{\Delta RING}$ transfected cells (Fig. 5A). Intriguingly, the levels of nuclear p50 subunit in XIAP$^{NLS\ C\text{-}term}$ were not similarly increased when compared to the other vectors (Supplementary Fig. 7). To verify whether changes in NF-κB expression and localization were accompanied by modulation in its transcriptional activity, we co-transfected each XIAP variant in HEK293 cells stably expressing a reporter to NF-κB in fusion with luciferase. Our results show that NF-κB transcriptional activity remained low and nearly unchanged in non-stimulated cells, but was clearly induced following stimulation with TNF-α (Fig. 5B). Remarkably, NF-κB luciferase activity was significantly reduced following transfections with XIAP^{H467A} and XIAP$^{\Delta RING}$ vectors, both of which lack ubiquitin ligase activity. This effect was partially reversed by transfection with XIAP$^{NLS\ C\text{-}term}$, which induced NFκB transcriptional activity in an extent similar to the wild-type form (Fig. 5B, right panel). These data suggest that the effects we observed in XIAP$^{NLS\ C\text{-}term}$ overexpressing cells are not related to IAP regulation but are likely to involve the NFκB pathway.

To investigate whether XIAP modulates polyubiquitin linkages, we focused on K48 and K63, the most abundant and functionally significant ubiquitin chains. Following transfections of MCF-7 cells with XIAP expression plasmids, we observed that K63-linked polyubiquitin chains were found more abundant in XIAP$^{NLS\ C\text{-}term}$ than in the other transfectants (Fig. 5C). Interestingly, no evident variations were

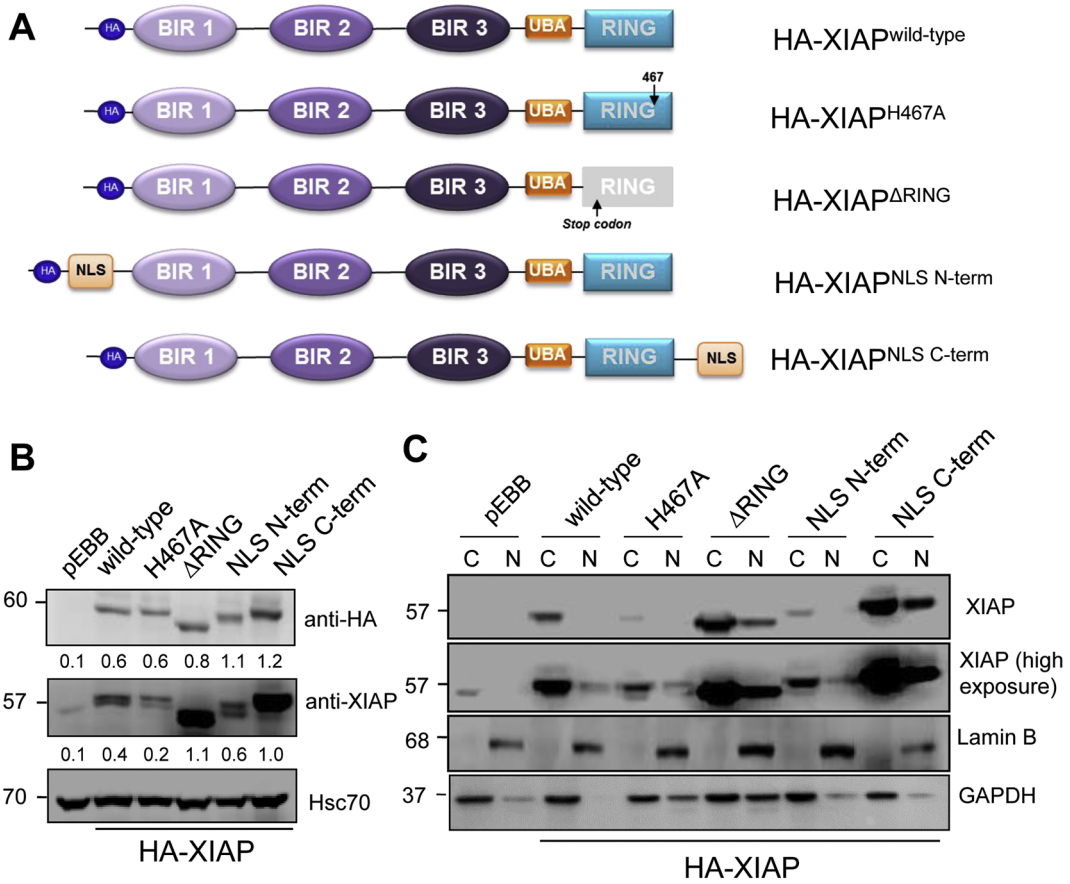

Fig. 2. XIAP expression and subcellular localization in MCF-7 cells overexpressing the vectors pEBB, XIAP$^{wild\ type}$, XIAP^{H467A}, XIAP$^{\Delta RING}$, XIAP$^{NLS\ N\text{-}term}$ and XIAP$^{NLS\ C\text{-}term}$. MCF-7 cells were left to adhere in petri dishes (10 cm) for 24 h and thereafter, were transfected with the pEBB, XIAP$^{wild\ type}$, XIAP^{H467A}, XIAP$^{\Delta RING}$, XIAP$^{NLS\ N\text{-}term}$ and XIAP$^{NLS\ C\text{-}term}$ vectors (A), using Lipofectamine 2000. (B) The levels of XIAP expression in XIAP-transfected cells were examined by Western blotting 24 h post-transfection. The relative expression levels of XIAP and HA-tag were determined based on the expression levels of the target gene product *versus* the reference, Hsc70. The values are shown below the respective Western blot bands (C) MCF-7 cells had their cytoplasmic and nuclear fractions separated by NE-PER kit (Thermoscientific) and XIAP expression was evaluated by Western blotting after 24 h of transfection. Lamin B and GAPDH were used as nuclear and cytoplasmic constitutive controls, respectively. C: cytoplasm; N: nucleus. (D) Following 24 h of transfection, MCF-7 cells overexpressing XIAP variants were submitted to the immunofluorescence protocol for XIAP (green) and anti-HA-tag (red) staining. Subcellular localization of XIAP was analyzed by confocal microscopy and nuclei were counterstained with DAPI. Scale bar: 10 and 20 μM.

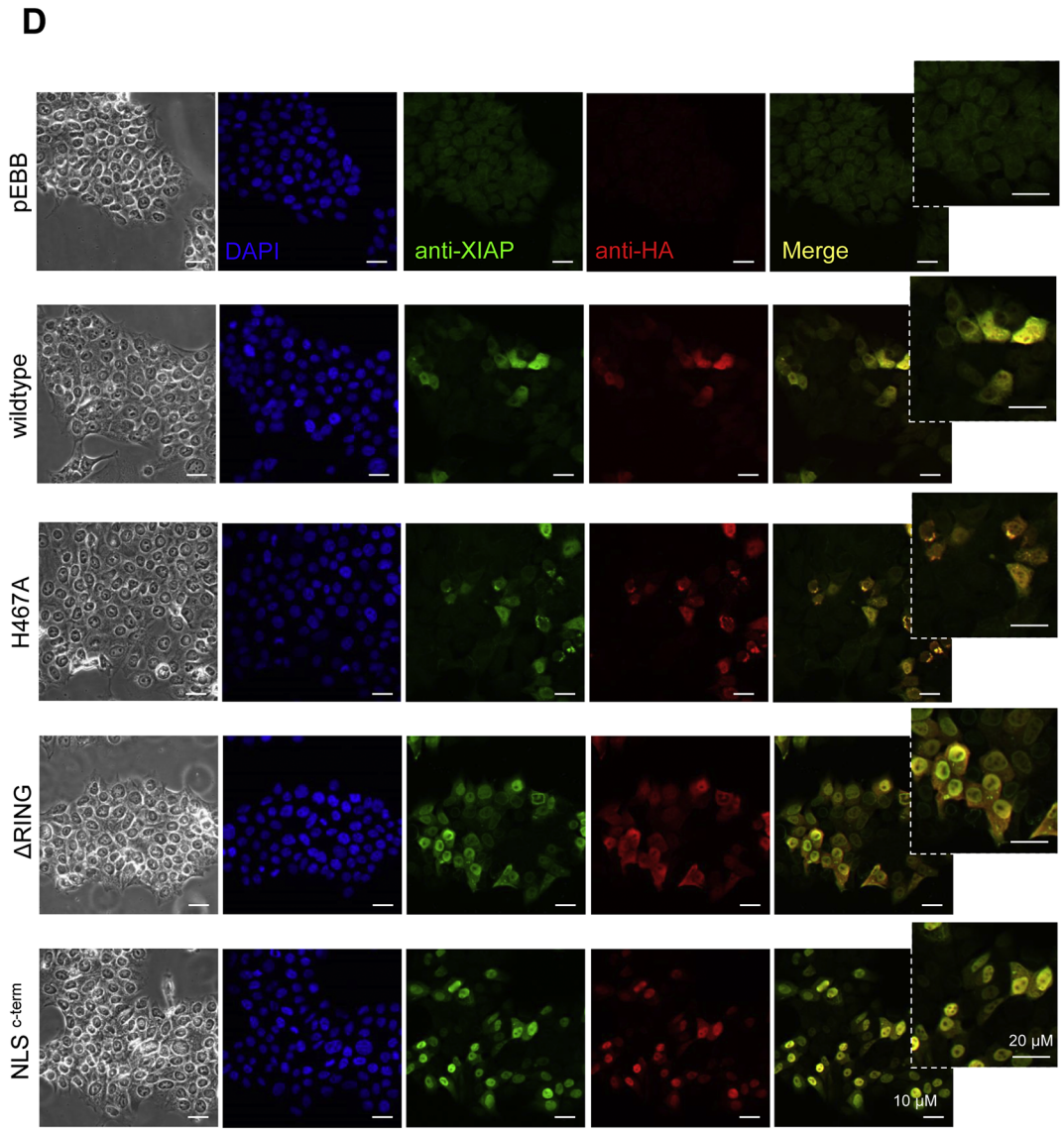

Fig. 2. (*continued*)

observed in the levels of K48-linked polyubiquitin chains within XIAP variants (Fig. 5C). These findings provide some mechanistic insights into XIAP functions and further suggest that XIAP$^{NLS\ C\text{-}term}$ might act to contribute to nuclear RING domain-dependent signal transduction instead of proteasome degradation of potential substrates.

3.6. Nuclear expression of XIAP is an independent predictor of poor prognosis in hormone receptor-negative breast cancer patients

In a previous work, we have labeled XIAP expression by immunohistochemistry in biopsies of 138 women with stage III ductal invasive carcinoma of the breast, in order to investigate the association between the expression of XIAP and FOXM1, an oncogenic transcription factor which transcriptionally regulates XIAP gene expression [8]. Herein, we aimed to explore the clinical significance of our findings concerning the association between nuclear XIAP and an aggressive phenotype *in vitro*. For this purpose, we deepened our analysis of XIAP expression and cellular distribution not only in the patient cohort as a whole, but also in breast cancer subtypes, where we observed three different XIAP distribution patterns: nuclear, both nuclear and cytoplasmic or cytoplasmic XIAP staining (Fig. 6A, B and C). When we stratified the patients into subgroups with distinct clinicopathological characteristics, such as high or low tumor grade, age below or above 50 years, each tumor size, each lymph node status, each IHC subtype and status of vascular invasion, no statistically significant associations were observed between expression and subcellular distribution of XIAP and patient overall survival in 10 years (data not shown). Nevertheless, univariate analysis of subgroups of patients positive and negative for HR revealed that expression of nuclear XIAP was significantly associated with poor prognosis in the HR-negative breast cancer patients (Fig. 6D). This finding was not confirmed for HR-positive cases neither total and cytoplasmic XIAP, whose expression pattern had no impact on patient survival (Supplementary Fig. 8A, B and C). Also, analysis from chi-square tests showed that, while cytoplasmic XIAP expression in HR-positive patients was associated with age above 50 years and low tumor grade, classical favorable prognostic factors for breast cancer (Supplementary Table 2), there were no significant associations between expression of nuclear XIAP in HR-positive patients and clinicopathological parameters, except for tumor size (Supplementary Table 3).

Next, we separately compared survival curves for patients exhibiting exclusively cytoplasmic XIAP (76 cases; 55%) and nuclear XIAP (18 cases; 13%), excluding those with simultaneous expression of nuclear and cytoplasmic XIAP (14 cases; 10%). Remarkably, patients expressing only nuclear XIAP presented significantly lower survival rates

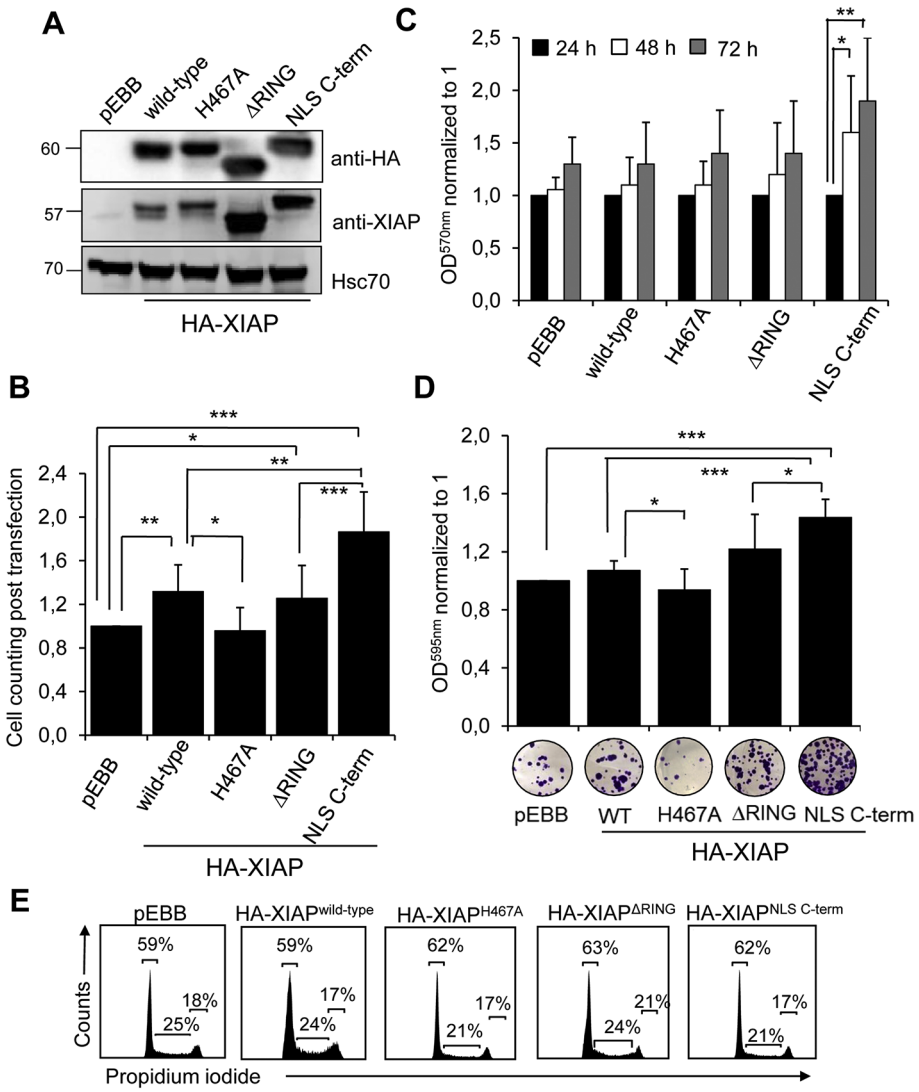

Fig. 3. Breast cancer cell growth profile in response to overexpression of XIAP and its mutants. (A) MCF-7 cells were left to adhere in petri dishes (10 cm) or, alternatively, in 6-well plates for 24 h and thereafter, were transfected with pEBB, XIAP$^{wild\ type}$, XIAP^{H467A}, XIAP$^{\Delta RING}$ and XIAP$^{NLS\ C\text{-}term}$ vectors using Lipofectamine 2000. (B) Transfected cells were counted *via* trypan blue exclusion 24 h post transfection. The total number of cells transfected with the empty vector (pEBB) in each experiment was normalized to the value of 1. The graph corresponds to means and standard deviation of five independent experiments (Student's *t*-test: $*p < 0.05$; $**p < 0.01$; $***p < 0.001$; considered statistically significant). (C) Cells were transfected and left to adhere in 96-well plate and cell mitochondrial viability was assessed at 24, 48 and 72 h. Optical density was obtained at 570 nm and values for each expression vector at 24 h were normalized to 1. The graph corresponds to means and standard deviation of three independent experiments (Student's *t*-test: $*p < 0.05$; $**p < 0.01$; considered statistically significant). (D) After 24 h of transfection, MCF-7 cells were left to adhere in 6-well plates for 24 h. Following colony formation, cells were stained with crystal violet and had their viability measured at 595 nm. The values obtained for cells transfected with the empty vector (pEBB) in each experiment were normalized to 1. The graph corresponds to the mean and standard deviation of four independent experiments (Student *t*-test: $*p < 0.05$; $**p < 0.01$; $***p < 0.001$; considered statistically significant). (E) The cell cycle profile of XIAP-overexpressing cells was evaluated by flow cytometry analysis of DNA content. The histograms are representative of three independent experiments.

than those expressing only cytoplasmic XIAP ($p = 0.012$) (Fig. 6E). This finding was restricted to the HR-negative group of patients, since we lacked biological significance of nuclear XIAP in the total population and in the group of HR-positive patients (Supplementary Fig. 9). Interestingly, survival curves for patients with concomitant expression of nuclear and cytoplasmic XIAP grouped with those with exclusive nuclear XIAP (Fig. 6F), suggesting that the clinical relevance of nuclear XIAP is irrespective of XIAP expression in the cytoplasm. We then questioned whether labeling of XIAP localization and HR expression could identify subgroups of breast cancer patients with distinct clinical outcomes. For this purpose, we stratified patients according to XIAP localization and HR status and compared survival curves by the log-rank test. Our results show that HR-negative patients with no expression of nuclear XIAP grouped with HR-positive patients in terms of overall survival rates (Fig. 6G). Conversely, we found that the survival curve reached statistical significance for lower survival rate in patients negative for HR exhibiting nuclear XIAP expression (Fig. 6G). This further suggests that labeling nuclear XIAP expression in breast cancer biopsies has the potential to identify a subgroup of poor outcome patients within the HR-negative specific group.

To further address the role of XIAP in breast cancer prognosis, we performed multivariate analysis of XIAP expression and localization and clinicopathological characteristics. Data from Cox regression model analysis showed that only the expression of HR was an independent predictor of prognosis in our cohort of patients (Table 1). When we stratified the cohort into groups with different HR status, we observed that expression of nuclear XIAP in HR-negative patients was an independent factor of unfavorable prognosis (Table 1), consistently with our previous results from univariate analysis. Altogether, this evidence indicates that the presence of nuclear XIAP in hormone-receptor negative patients leads to a reduced overall survival and might be used as a potential biomarker for prognosis in breast cancer.

4. Discussion

XIAP expression has been reported in different subcellular compartments [6], but a predominant cytoplasmic distribution in both cancer and normal tissues has been attributed to its role in caspase regulation. However, the analysis XIAP expression in breast cancer tissues revealed that XIAP can be detected at both nuclear and cytoplasmic compartments [8,9]. Since the differential role of XIAP across subcellular compartments has been poorly explored, we herein aimed at investigating how nuclear XIAP contributes to aggressive features in breast cancer. Data from cellular transfections with vectors encoding wild-type and mutant forms of XIAP revealed that XIAP$^{NLS\ C\text{-}term}$ and XIAP$^{\Delta RING}$ overexpressing cells exhibited nuclear XIAP apart from cytoplasmic XIAP, already present in MCF-7 cells. Interestingly, the overexpression of XIAP$^{NLS\ N\text{-}term}$ was not followed by XIAP nuclear localization, which suggests that the insertion of an NLS in the N-terminal end of XIAP might have resulted in conformational changes leading to

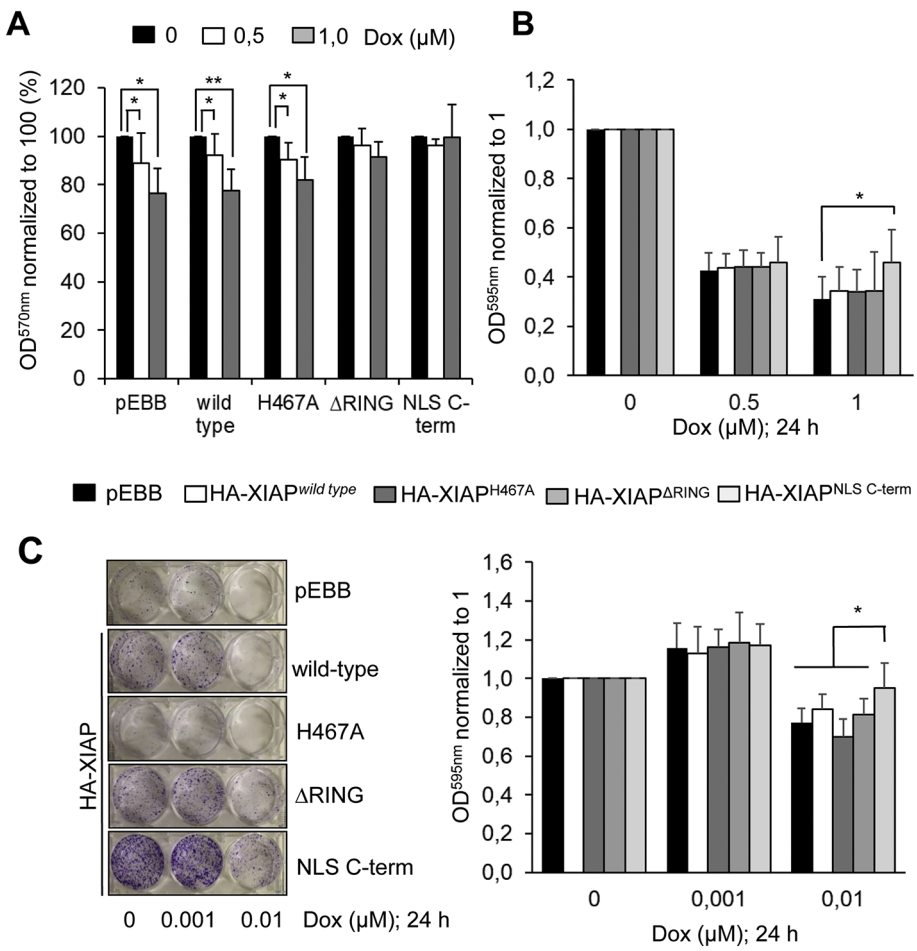

Fig. 4. Effect of overexpression of XIAP and its mutants on doxorubicin (dox) resistance in breast cancer cells. MCF-7 cells were left to adhere in petri dishes (10 cm) or, alternatively, in 6-well plates for 24 h and thereafter, were transfected with the vectors pEBB, XIAP$^{wild\ type}$, XIAP^{H467A}, XIAP$^{\Delta RING}$ and XIAP$^{NLS\ C\text{-}term}$, using Lipofectamine 2000. (A) After 24 h of transfection, MCF-7 cells were left to adhere in 96-well plates for 24 h. Subsequently, dox was added at 0.5 and 1 μM concentrations and the cells were incubated for 24 h for MTT assay. Cell viability was measured at 570 nm. The cell lines transfected with the different XIAP-encoding plasmids had each dox concentration compared to the control of untreated cells. (B) Cells were transfected and left to adhere in 96-well plate. After 24 h of drug exposure, they were fixed and stained with crystal violet and had their viability measured at 595 nm. The cell lines transfected with the different XIAP-encoding plasmids were compared to the empty vector pEBB, for each dox concentration. (C) After 24 h of transfection, MCF-7 cells were left to adhere in 6-well plates for 24 h. The cells were treated with dox for 24 h and left for 14 days in the CO_2 incubator. After colony formation, cells were stained with crystal violet and had their viability measured at 595 nm. All graphs correspond to means and standard deviation of three independent experiments (Student *t*-test: $*p < 0.05$; $**p < 0.01$, considered statistically significant).

masking of residues essential for importing recognition. The nuclear localization of XIAP$^{\Delta RING}$ overexpressing cells is consistent with data from [13], which reported the same subcellular distribution in a model of colorectal cancer cells. The reason behind the nuclear translocation of XIAP from the cytoplasm to the nucleus following the deletion of the RING domain remains to be determined. Interestingly, we performed a nuclear export signal (NES) prediction analysis of XIAP sequence at the NetNES 1.1 Server [17] and identified two hydrophobic residues located at the border and within the RING domain (Supplementary Fig. 10). Therefore, it is likely that the RING deletion prevents, at least in part, XIAP export to the cytoplasm, disrupting the balance in XIAP nuclear-cytoplasmic shuttling and leading to the nuclear accumulation of XIAP.

From functional assays with XIAP variants, we found that overexpression of XIAP$^{NLS\ C\text{-}term}$, but not XIAP$^{\Delta RING}$, was associated with improved cell count, clonogenicity capacity and cellular mitochondrial viability. Of note, XIAP$^{\Delta RING}$ overexpressing cells exhibited a proliferative capacity similar to XIAP$^{wild\text{-}type}$, which presented exclusive cytoplasmic XIAP. We also assessed the impact of XIAP transfectants in the acquisition of a drug resistance phenotype in drug-sensitive MCF-7 cells. Consistently, overexpression of XIAP$^{NLS\ C\text{-}term}$ partially reduced the response rates when cells were treated with clinically relevant concentrations of doxorubicin. Of note, our data from breast cell lines derived from distinct molecular subtypes associates exclusive cytoplasmic XIAP with a sensitive phenotype towards doxorubicin and even, paclitaxel. Also, we found no alterations in XIAP subcellular distribution following drug treatment, contrasting data from [18], which have shown that XIAP is translocated to the nucleus of lymphoma cells upon apoptotic stimuli induced by a wide range of chemotherapeutic agents with different modes of action. XIAP has also been shown to translocate into the nucleus in models of induced brain ischemia [19,20]. In these experimental settings, the sequestration of XIAP in nuclear inclusions was associated with the suppression of its ability to bind caspases and thus, with the increment in apoptotic cell death. Considering that nuclear XIAP is also associated with cancer cell growth in our breast cancer model and in colorectal cancer [13], it is likely that the biological roles played by XIAP in the nuclear compartment are dynamic, context-dependent and tissue-specific.

The mechanisms underlying XIAP translocation and effects induced in the nucleus are poorly understood. Since XIAP does not present an NLS in its sequence, it is supposed to shuttle from the cytoplasm to the nucleus through interacting with cargo proteins. Once in the nucleus, little is known on XIAP-mediated downstream effects on cell growth and drug resistance. Although nuclear XIAP expression is detected at similar levels in both XIAP$^{\Delta RING}$ and XIAP$^{NLS\ C\text{-}term}$ overexpressing cells, only XIAP$^{NLS\ C\text{-}term}$ promoted a cell growth advantage and a more chemoresistance phenotype compared to the wild type form of XIAP. These findings suggest that the C-terminal end of nuclear XIAP is required for XIAP-mediated aggressive features in our model of breast cancer cells. Although we cannot assume that the ubiquitin ligase function of the RING domain is intact following the insertion of an NLS in the C-terminal end of XIAP in XIAP$^{NLS\ C\text{-}term}$ overexpressing cells, nuclear XIAP-mediated effects might occur in a RING-dependent fashion. Notably, the RING domain of XIAP has also been implicated in bladder cancer transformation *via* the inhibition of p63α protein translation [21]. As a RING domain containing protein, XIAP acts like a ubiquitin E3 ligase and attaches ubiquitin to itself and target proteins [22]. Interestingly, overexpression of XIAP$^{NLS\ C\text{-}term}$ was associated with an increase in K63 polyubiquitin chains. Conversely, the levels of K48 chains remain unchanged, indicating that XIAP$^{NLS\ C\text{-}term}$-induced

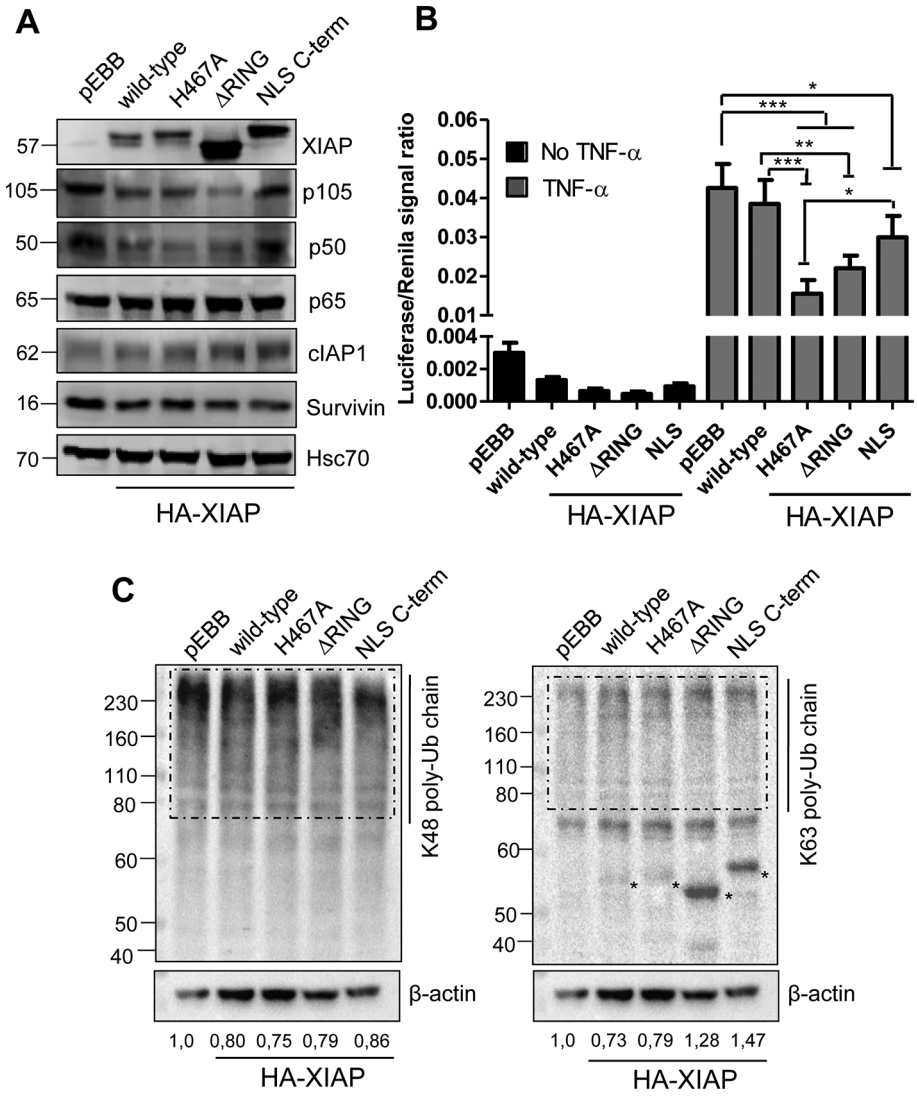

Fig. 5. NFκB transcriptional activity and expression profile of K63 and K48-linked ubiquitination, NFκB subunits, Survivin and cIAP1 upon overexpression of mutant forms of XIAP. MCF-7 cells were left to adhere in petri dishes (10 cm) for 24 h and thereafter, were transfected with the pEBB, $XIAP^{wild\ type}$, $XIAP^{H467A}$, $XIAP^{\Delta RING}$ and $XIAP^{NLS\ C\text{-}term}$ vectors, using Lipofectamine 2000. (A) The expression levels of XIAP, NFκB subunits (p50, p105 and p65), cIAP1 and Survivin were examined by Western blotting from whole cell lysates obtained from XIAP-transfected cells. (B) HEK293 cells expressing a NF-κB reporter gene in fusion with firefly luciferase was transfected with indicated plasmids in addition to renilla luciferase plasmid to be used as transfection normalization. They were treated or not with 10 ng/mL TNF-alpha during 12 h and lysed to luminescence quantification of firefly and renilla luciferase. The ratio of firefly/renilla luciferase was used to plot the graphs. The graph corresponds to means and standard deviation of five independent experiments (two-way ANOVA: $*p < 0.05$; $**p < 0.01$; $***p < 0.005$). (C) The expression pattern of K63 and K48 poly-ubiquitin chains were measured by Western blotting using K63 and K48-specific antibodies and quantification of ubiquitination was carried out from a smear of 80 until 230 kDa band (densitometry from the dashed area) following normalization against β-actin levels. The values are shown below the respective Western blot bands. The asterisks indicate unspecific bands.

oncogenic functions are not related to target proteasomal degradation and might be linked to signaling transduction. Increasing evidence suggests that XIAP leads to upregulation of canonical Wnt signaling through the ubiquitination of its negative regulator Groucho/TLE in the nucleus [23,24]. In $XIAP^{\Delta RING}$ overexpressing colorectal cancer cells, nuclear XIAP interacts with E2F1 transcription factor *via* its BIR domain to promote cyclin-E expression and induce anchorage-independent growth [13]. Corroborating these data, overexpression of XIAP deleted for the RING domain in bladder cancer cells promoted EGFR translation through a PP2A/MAPK/JNK signaling pathway leading to the suppression of microRNA-200a and anchorage-independent growth [25]. This indicates that XIAP might exert RING-dependent and independent functions in the nucleus across distinct cellular models. We herein have also investigated molecular pathways known to crosstalk with XIAP and found that XIAP-induced effects are independent on Survivin and cIAP-1 expression, but might involve increased p50 protein content and NF-κB transcriptional activity. NF-κB activation by XIAP can either involve the RING [10], the UBA [26] or BIR [27] domains of XIAP. Of note, most data on the role of XIAP overexpression in biological processes have been obtained from PCR or Western blotting data from whole cells pellets. However, increasing evidence suggests that addressing XIAP subcellular distribution might be equally important. Our study adds to this emerging literature and encourages the analysis of XIAP expression in different cellular compartments as a way towards refining the identification of its molecular mechanisms and biological functions beyond the regulation of apoptosis.

To further validate the biological relevance of our *in vitro* findings, we strengthened our analysis of XIAP subcellular distribution in patients with invasive ductal carcinoma of the breast. In our previous study, we obtained a percentage of 78.3% XIAP positivity, among which 91 cases presented cytoplasmic (65.9%) and 31 nuclear XIAP expression (22.5%). However, we found no association between individual expression of total (cytoplasmic and/or nuclear), cytoplasmic or nuclear XIAP with patient poor outcome in univariate analysis [8]. However, considering the heterogeneity in breast cancer, it is crucial to investigate biomarkers in subgroups of patients from distinct molecular subtypes. The stratification of our cohort into subgroups with different clinical-biological characteristics revealed that nuclear XIAP has an impact in HR negative patients, but not in any other subgroup. We confirmed these data in multivariate analysis, where we found nuclear expression of XIAP as an independent predictor of poor prognosis. This particular finding is consistent with a report from [9], but contrasts [28], which could not find an independent impact for nuclear XIAP. More importantly, labelling nuclear XIAP in our patients could identify a subpopulation with unfavorable clinical prognosis. Remarkably, patients who did not exhibit nuclear XIAP presented survival curves grouped with HR positive patients, a good prognosis subtype. Our findings on the prognostic value of nuclear XIAP expression in HR negative patients are quite important, considering the scarce therapeutic opportunities directed to this subgroup of patients. Of note, treatment

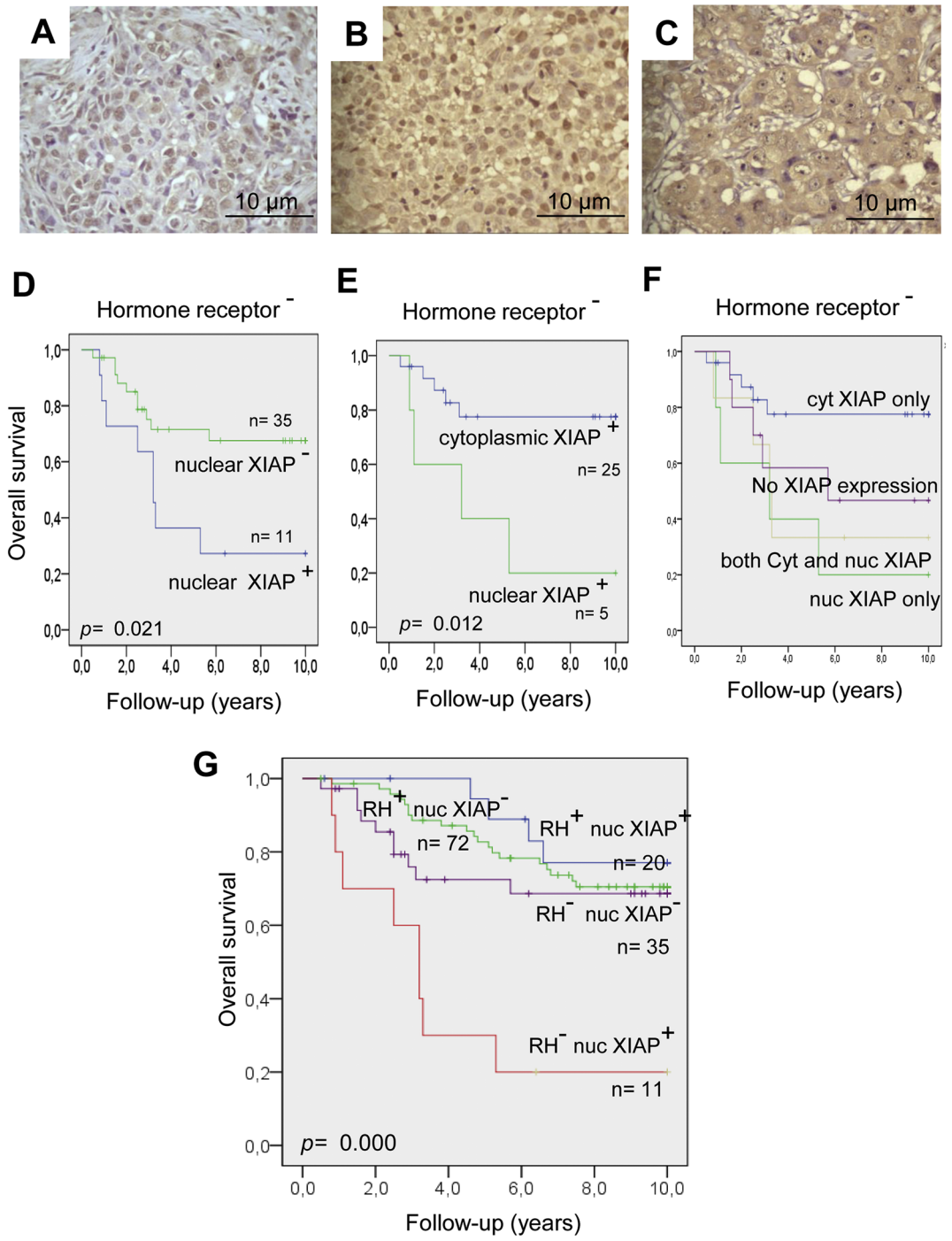

Fig. 6. Overall survival of patients with infiltrating ductal breast carcinoma grouped according to cytoplasmic or nuclear expression of XIAP. Representative staining from immunohistochemical analysis of XIAP expression: Nuclear XIAP staining scored 8 (A). Both nuclear and cytoplasmic XIAP staining scored 6 and 8, respectively (B). Cytoplasmic XIAP staining scored 8 (C). Original magnification 40×; scale bar 10 µM. (D, E, F) The impact of XIAP subcellular localization was analyzed in the hormone receptor-negative subgroups. (G) The impact of XIAP subcellular localization in the total population was analyzed according to expression of nuclear XIAP and hormone receptors. The Kaplan-Meier curves, were compared by the log-rank test, where the value of $p < 0.05$ was considered statistically significant. HR: hormone receptors; Cyt: cytoplasmic; Nuc: nuclear.

protocols for these patients are generally based on the combination of anthracyclines and taxanes and associated with low complete response rates [29]. The better understanding of the mechanisms of XIAP translocation from the cytoplasm to the nucleus might shed light into the design of potential novel strategies aiming at preventing or inhibiting XIAP expression specifically at the nuclear compartment of breast cancer cells.

To sum up, our study is the first to report the mechanisms and effects associated with XIAP localization in the nucleus of breast cancer cells. Our findings suggest that nuclear XIAP associates with poor clinical outcome in HR-negative breast cancer patients as well as promotes cell growth and drug resistance *in vitro* in a RING-associated fashion, further contributing towards an aggressive phenotype in this neoplasm. XIAP overexpression has been widely implicated in cancer

Table 1
Multivariate analysis of XIAP expression and localization and breast cancer prognostic factors.

Characteristics	Total population			Hormone receptor-positive patients			Hormone receptor-negative patients		
	Multivariate analysis								
	p	HR	(95% CI)	*p*	HR	(95% CI)	*p*	HR	(95% CI)
Age at diagnosis	0.814	0.055	(0.964–1.048)	0.569	0.569	(0.933–1.039)	0.409	0.682	(0.957–1.114)
Tumor size	0.631	0.231	(0.583–1.386)	0.767	0.088	(0.640–1.389)	0.206	1600	(0.181–1.446)
Tumor grade	0.340	0.912	(0.686–2.987)	0.498	0.459	(0.504–4.089)	0.061	3497	(0.910–55.629)
Her2 expression	0.161	1964	(0.556–34.298)	0.986	0.000	(0.000–)	0.560	0.340	(0.184–22,867)
Hormone receptors	0.023	5167	(1.140–5.878)	–	–	–	–	–	–
Total XIAP expression	0.756	0.097	(0.264–6.333)	0.406	0.691	(0.024–4.503)	0.326	0.966	0.223–92.968)
Cytoplasmic XIAP	0.720	0.128	(0.334–4.894)	0.554	0.351	(0.198–20.574)	0.669	0.183	(0.174–15.216)
Nuclear XIAP	0.358	0.846	(0.175–1.875)	0.567	0.328	(0.231–14.459)	0.011	6504	(0.004–0.483)

drug resistance, mainly through its BIR domains through which it exerts its caspase-inhibitory activities, mainly at the cytoplasm. The potential relevance of the RING domain in the effects mediated by nuclear XIAP suggests the identification of RING-directed therapeutic strategies to circumvent not only cytoplasmic but also nuclear XIAP functions. Finally, our data on the role of nuclear XIAP as an independent prognostic factor, capable of identifying a population within HR negative patients with even worse clinical outcomes, denote the prognostic value and clinical utility of analyzing not only XIAP overexpression, but also subcellular distribution.

Supplementary data to this article can be found online at https://doi.org/10.1016/j.bbamcr.2020.118761.

CRediT authorship contribution statement

Deborah Delbue:Conceptualization, Methodology, Formal analysis, Investigation, Writing - original draft, Visualization.**Bruna S. Mendonça**:Methodology, Validation, Formal analysis, Investigation, Writing - original draft, Visualization.**Marcela C. Robaina**:Methodology, Investigation, Formal analysis.**Lauana G.T. Lemos**:Methodology, Formal analysis.**Pedro I. Lucena**: Methodology, Investigation, Writing - review & editing.**João P.B. Viola**:Resources, Writing - review & editing, Funding acquisition.**Lídia M. Magalhães**:Methodology, Investigation. **Susanne Crocamo**:Resources, Writing - review & editing.**Caio A.B. Oliveira**:Methodology, Formal analysis.**Felipe R. Teixeira**: Investigation, Resources, Formal analysis, Writing - review & editing, Visualization, Funding acquisition.**Raquel C. Maia**: Investigation, Resources, Writing - review & editing, Funding acquisition.**Gabriela Nestal de Moraes**:Conceptualization, Methodology, Validation, Investigation, Resources, Formal analysis, Writing - original draft, Visualization, Supervision, Project administration, Funding acquisition.

Declaration of competing interest

The authors declare no conflicts of interest.

Acknowledgements

We would like to thank Professor Colin Duckett (University of Michigan, USA) for kindly providing the expression vectors pEBB (empty vector), pEBB-HA-XIAP$^{wild\ type}$, pEBB-HA-XIAP^{H467A} (loss of ubiquitin E3 ligase function) and pEBB-HA-XIAP$^{\Delta RING}$ used in this study. We are also grateful to Dr. Matheus Rajão for his excellent technical assistance with the confocal microscopy and Dr. Claudete Klumb for valuable discussions on the data. We should also thank Dr. Maria Theresa Accioly for her support with the patient samples.

Funding

G.N. was supported by funds from Fundação de Amparo à Pesquisa do Estado do Rio de Janeiro (FAPERJ, grant number E-26/010.001808/2016), L'óreál-UNESCO-ABC Para Mulheres na Ciência (L'óreál for women in science) and the Brazilian National Cancer Institute – Ministry of Health (INCA-MS). R.C.M. was supported by Conselho Nacional de Desenvolvimento Científico e Tecnológico (CNPq) Produtividade (grant number 304565/2016-4). C.A.B.O. and F.R.T. were supported by FAPESP (2016/21310-6) and FAPESP grant number 2016/25798-3. The funding agencies had no involvement in the study design, data collection and writing.

References

[1] A.J. Kocab, C.S. Duckett, Inhibitor of apoptosis proteins as intracellular signaling intermediates, FEBS J. 283 (2016) 221–231.
[2] F.L. Scott, J.B. Denault, S.J. Riedl, H. Shin, M. Renatus, G.S. Salvesen, XIAP inhibits caspase-3 and -7 using two binding sites: evolutionarily conserved mechanism of IAPs, EMBO J. 24 (2005) 645–655.
[3] Y. Yang, S. Fang, J.P. Jensen, A.M. Weissman, J.D. Ashwell, Ubiquitin protein ligase activity of IAPs and their degradation in proteasomes in response to apoptotic stimuli, Science 288 (2000) 874–877.
[4] Y. Suzuki, Y. Nakabayashi, R. Takahashi, Ubiquitin-protein ligase activity of X-linked inhibitor of apoptosis protein promotes proteasomal degradation of caspase-3 and enhances its anti-apoptotic effect in Fas-induced cell death, Proc. Natl. Acad. Sci. U. S. A. 98 (2001) 8662–8667.
[5] M. MacFarlane, W. Merrison, S.B. Bratton, G.M. Cohen, Proteasome-mediated degradation of Smac during apoptosis: XIAP promotes Smac ubiquitination in vitro, J. Biol. Chem. 277 (2002) 36611–36616.
[6] B. Vischioni, P. van der Valk, S.W. Span, F.A. Kruyt, J.A. Rodriguez, G. Giaccone, Expression and localization of inhibitor of apoptosis proteins in normal human tissues, Hum. Pathol. 37 (2006) 78–86.
[7] M.S. Mohamed, M.K. Bishr, F.M. Almutairi, A.G. Ali, Inhibitors of apoptosis: clinical implications in cancer, Apoptosis 22 (2017) 1487–1509.
[8] G. Nestal de Moraes, D. Delbue, K.L. Silva, M.C. Robaina, P. Khongkow, A.R. Gomes, S. Zona, S. Crocamo, A.L. Mencalha, L.M. Magalhaes, E.W. Lam, R.C. Maia, FOXM1 targets XIAP and Survivin to modulate breast cancer survival and chemoresistance, Cell. Signal. 27 (2015) 2496–2505.
[9] Y. Zhang, J. Zhu, Y. Tang, F. Li, H. Zhou, B. Peng, C. Zhou, R. Fu, X-linked inhibitor of apoptosis positive nuclear labeling: a new independent prognostic biomarker of breast invasive ductal carcinoma, Diagn. Pathol. 6 (2011) 49.
[10] J. Lewis, E. Burstein, S.B. Reffey, S.B. Bratton, A.B. Roberts, C.S. Duckett, Uncoupling of the signaling and caspase-inhibitory properties of X-linked inhibitor of apoptosis, J. Biol. Chem. 279 (2004) 9023–9029.
[11] G. Nestal de Moraes, F.C. Vasconcelos, D. Delbue, G.P. Mognol, C. Sternberg, J.P. Viola, R.C. Maia, Doxorubicin induces cell death in breast cancer cells regardless of Survivin and XIAP expression levels, Eur. J. Cell Biol. 92 (2013) 247–256.
[12] E. Kopp, R. Medzhitov, J. Carothers, C. Xiao, I. Douglas, C.A. Janeway, S. Ghosh, ECSIT is an evolutionarily conserved intermediate in the Toll/IL-1 signal transduction pathway, Genes Dev. 13 (1999) 2059–2071.
[13] Z. Cao, X. Li, J. Li, W. Luo, C. Huang, J. Chen, X-linked inhibitor of apoptosis protein (XIAP) lacking RING domain localizes to the nuclear and promotes cancer cell anchorage-independent growth by targeting the E2F1/Cyclin E axis, Oncotarget 5 (2014) 7126–7137.
[14] P. Obexer, M.J. Ausserlechner, X-linked inhibitor of apoptosis protein — a critical death resistance regulator and therapeutic target for personalized cancer therapy, Front. Oncol. 4 (2014) 197.

[15] R. Hofer-Warbinek, J.A. Schmid, C. Stehlik, B.R. Binder, J. Lipp, R. de Martin, Activation of NF-kappa B by XIAP, the X chromosome-linked inhibitor of apoptosis, in endothelial cells involves TAK1, J. Biol. Chem. 275 (2000) 22064–22068.
[16] T. Dohi, K. Okada, F. Xia, C.E. Wilford, T. Samuel, K. Welsh, H. Marusawa, H. Zou, R. Armstrong, S. Matsuzawa, G.S. Salvesen, J.C. Reed, D.C. Altieri, An IAP-IAP complex inhibits apoptosis, J. Biol. Chem. 279 (2004) 34087–34090.
[17] T. la Cour, L. Kiemer, A. Molgaard, R. Gupta, K. Skriver, S. Brunak, Analysis and prediction of leucine-rich nuclear export signals, Protein Eng. Des. Sel. 17 (2004) 527–536.
[18] D. Nowak, S. Boehrer, A. Brieger, S.Z. Kim, S. Schaaf, D. Hoelzer, P.S. Mitrou, E. Weidmann, K.U. Chow, Upon drug-induced apoptosis in lymphoma cells X-linked inhibitor of apoptosis (XIAP) translocates from the cytosol to the nucleus, Leuk. Lymph. 45 (2004) 1429–1436.
[19] M. Siegelin, O. Touzani, J. Toutain, P. Liston, A. Rami, Induction and redistribution of XAF1, a new antagonist of XIAP in the rat brain after transient focal ischemia, Neurobiol. Dis. 20 (2005) 509–518.
[20] J.C. Russell, H. Whiting, N. Szuflita, M.A. Hossain, Nuclear translocation of X-linked inhibitor of apoptosis (XIAP) determines cell fate after hypoxia ischemia in neonatal brain, J. Neurochem. 106 (2008) 1357–1370.
[21] H. Jin, J. Xu, X. Guo, H. Huang, J. Li, M. Peng, J. Zhu, Z. Tian, X.R. Wu, M.S. Tang, C. Huang, XIAP RING domain mediates miR-4295 expression and subsequently inhibiting p63alpha protein translation and promoting transformation of bladder epithelial cells, Oncotarget 7 (2016) 56540–56557.
[22] R. Budhidarmo, C.L. Day, IAPs: modular regulators of cell signalling, Semin. Cell Dev. Biol. 39 (2015) 80–90.
[23] A.J. Hanson, H.A. Wallace, T.J. Freeman, R.D. Beauchamp, L.A. Lee, E. Lee, XIAP monoubiquitylates Groucho/TLE to promote canonical Wnt signaling, Mol. Cell 45 (2012) 619–628.
[24] V.H. Ng, B.I. Hang, L.M. Sawyer, L.R. Neitzel, E.E. Crispi, K.L. Rose, T.M. Popay, A. Zhong, L.A. Lee, W.P. Tansey, S. Huppert, E. Lee, Phosphorylation of XIAP at threonine 180 controls its activity in Wnt signaling, J. Cell Sci. 131 (2018).
[25] C. Huang, X. Zeng, G. Jiang, X. Liao, C. Liu, J. Li, H. Jin, J. Zhu, H. Sun, X.R. Wu, C. Huang, XIAP BIR domain suppresses miR-200a expression and subsequently promotes EGFR protein translation and anchorage-independent growth of bladder cancer cell, J. Hematol. Oncol. 10 (2017) 6.
[26] M. Gyrd-Hansen, M. Darding, M. Miasari, M.M. Santoro, L. Zender, W. Xue, T. Tenev, P.C. da Fonseca, M. Zvelebil, J.M. Bujnicki, S. Lowe, J. Silke, P. Meier, IAPs contain an evolutionarily conserved ubiquitin-binding domain that regulates NF-kappaB as well as cell survival and oncogenesis, Nat. Cell Biol. 10 (2008) 1309–1317.
[27] M. Lu, S.C. Lin, Y. Huang, Y.J. Kang, R. Rich, Y.C. Lo, D. Myszka, J. Han, H. Wu, XIAP induces NF-kappaB activation via the BIR1/TAB1 interaction and BIR1 dimerization, Mol. Cell 26 (2007) 689–702.
[28] Y.C. Xu, Q. Liu, J.Q. Dai, Z.Q. Yin, L. Tang, Y. Ma, X.L. Lin, H.X. Wang, Tissue microarray analysis of X-linked inhibitor of apoptosis (XIAP) expression in breast cancer patients, Med. Oncol. 31 (2014) 764.
[29] A.C. Garrido-Castro, N.U. Lin, K. Polyak, Insights into molecular classifications of triple-negative breast cancer: improving patient selection for treatment, Cancer Discov. 9 (2019) 176–198.